Supplementary Information

Supplementary Figures

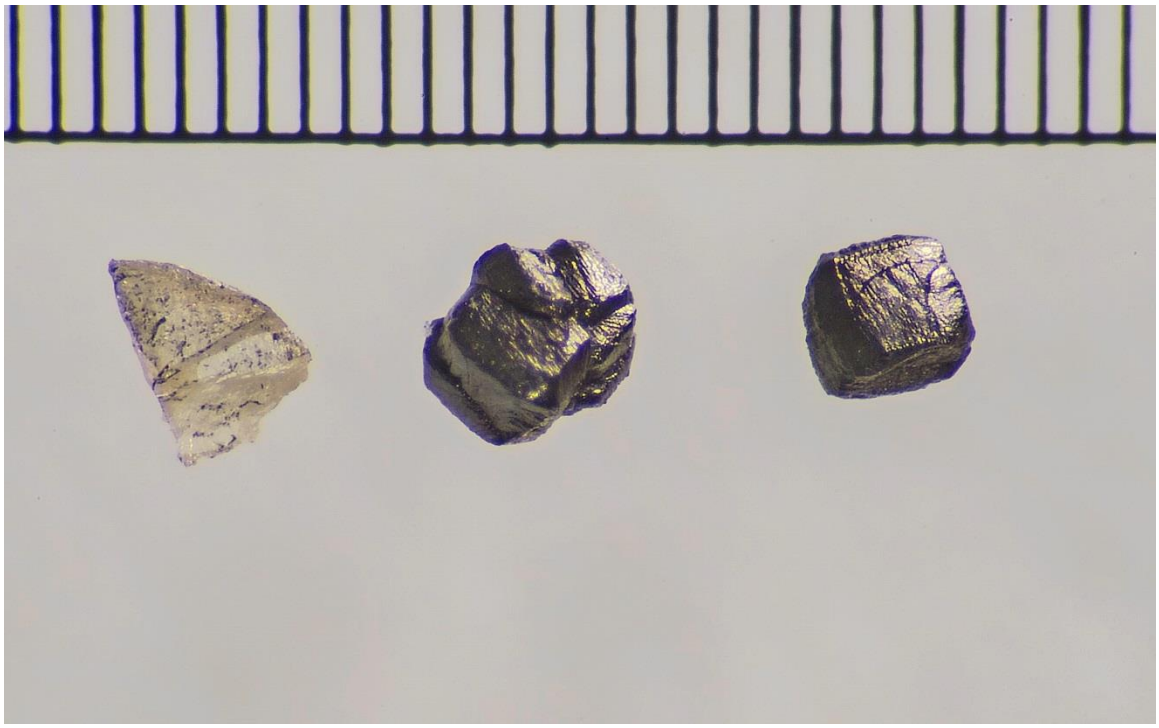

Supplementary Figure 1 Grains from the synthetic (clear) and Canyon Diablo (black) samples. Tick marks on the scale bar = 200 microns.

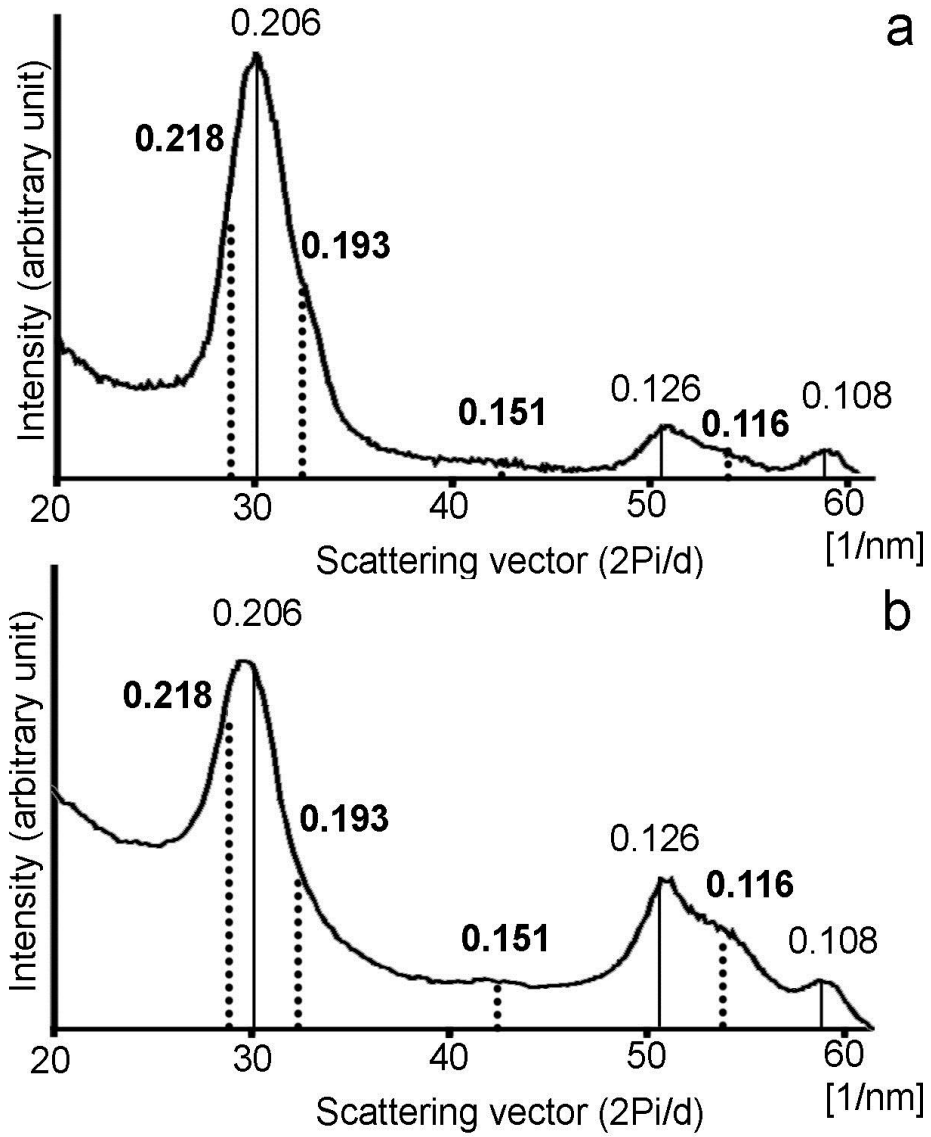

Supplementary Figure 2 Radial distributions of SAED intensities. They match the profile of the XRD pattern and show the diffraction features attributed to "lonsdaleite." **a)** Data generated from Fig. 1b. **b)** Data generated from Fig. 1c. The d-spacings attributed to lonsdaleite are indicated by vertical dotted lines and bold numbers. The positions of the peaks in the radial distributions (**a**, **b**) and XRD patterns (Fig. 1a) are similar but display small intensity differences. In particular, along <121> projection (**b**) the relative intensity of the 0.126-nm diffraction peak is strong and the 0.193-nm shoulder on the 0.206 peak is weak. The intensity differences are explained by differences in (1) the scattering efficiencies of electrons versus X-rays, (2) broadening of the X-ray and electron-diffraction peaks, and (3) orientation. Radial distributions of intensities were generated from Figs 1b and c following the method described by (ref. 1) and using the ProcessDiffraction software. The distributions were calibrated by assigning the second strongest peak to the *d*-value of 0.126 nm, which is the same for both diamond and "lonsdaleite."

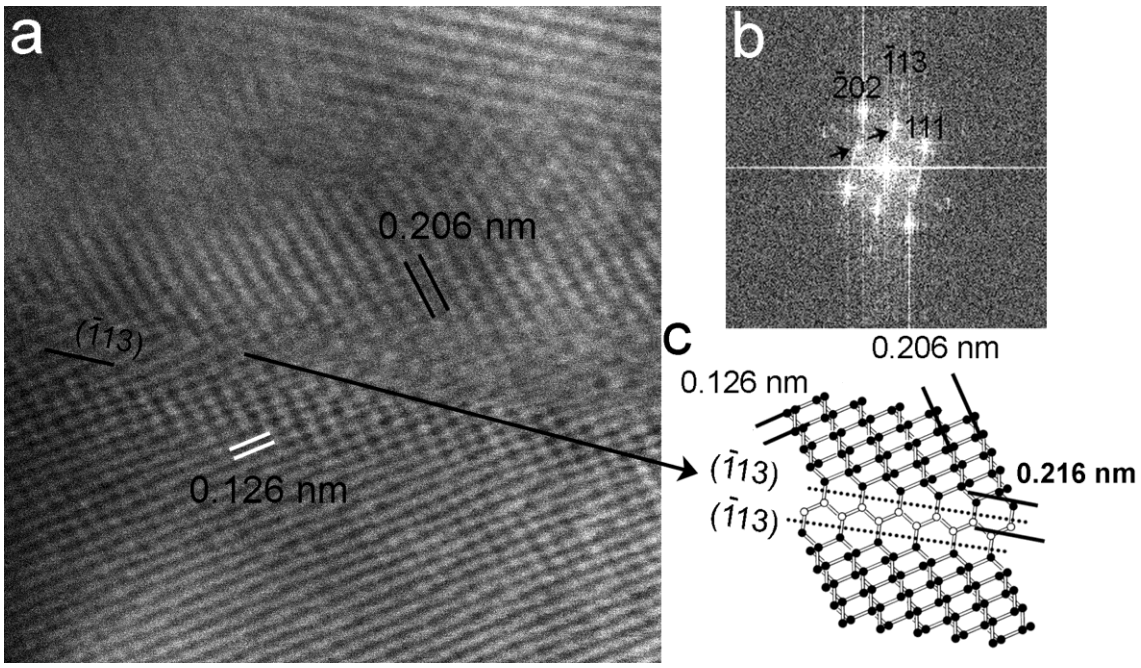

Supplementary Figure 3 Evidence for Mechanism II from the synthetic sample. {113} twins from the synthetic sample (<121> projection) provide an explanation for the hexagonally arranged reflections and 0.216-nm spacings attributed to "lonsdaleite." **a)** High-resolution STEM image. **b)** FFT calculated from **a**. Black arrows mark hexagonally arranged reflections absent in single-crystal diamond. **c)** Structure model across the {113} twins.

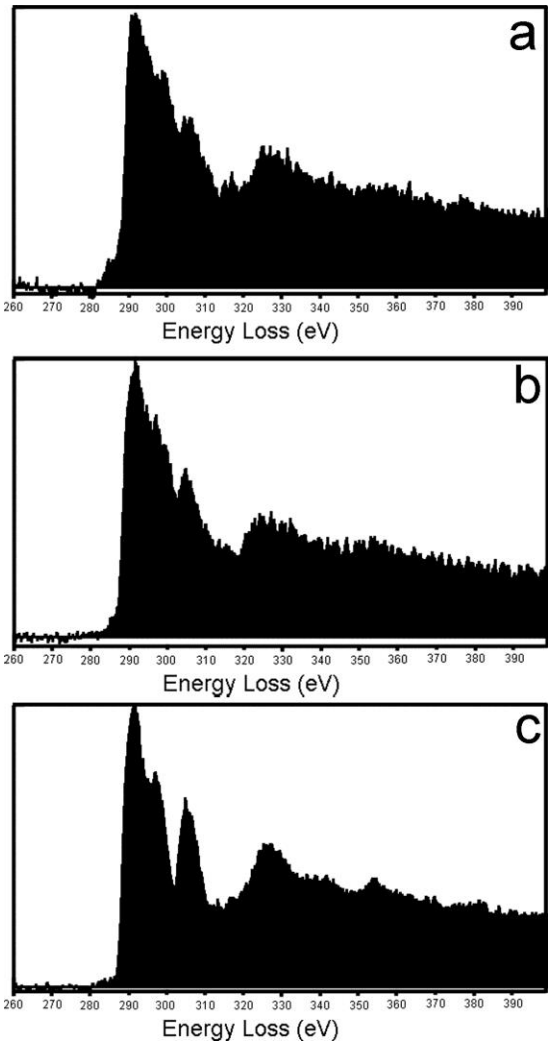

Supplementary Figure 4 EELS data. a) Acquired from the whole area of Fig. 2c. **b)** Acquired from the whole area of Fig. 4a. **c)** Acquired from a piece of cubic diamond from Minas Gerais (Brazil). The carbon *K* edges of **a** and **b** are consistent with those of **c**. The broader peaks in **a** and **b**, relative to **c**, likely arise from the abundant defects in the analyzed region. The decrease in intensity of the peak around 305 eV following the second absolute band gap at 302 eV relative to pristine diamond results from the decrease in the ideal diamond lattice structure such as from defect state (ref. 2 and references therein). Reduction in intensity of the 305 eV peak in **a** and **b** relative to **c** (pristine diamond) is therefore attributed to the high density of defects and lack of long-range order. A power-law background was subtracted from beneath the C K edges.

Supplementary Note 1

Controversial diagnostic signatures of "lonsdaleite"

The sp^3 Raman bands between 1200-1400 cm^{-1} are not unique for "lonsdaleite," but there is considerable overlap with those of graphite and diamond[3]. Although an sp^3 Raman band at 1324 cm^{-1} has been proposed[3] as characteristic of "lonsdaleite,", this band is broad with intensity orders of magnitude lower than that of diamond at 1332 cm^{-1} and thus cannot be unambiguously attributed to a pure phase containing only sp^3-bonded carbon. Furthermore, the Raman band at 1324 cm^{-1} may also result from some carbon-based impurity in the product of the shock experiment[3]. The carbon *K* edge EELS peaks at 310 and 330 eV have also been used to identify "lonsdaleite" [4], but these peaks also match those of diamond (see Supplementary Figure 4c). Furthermore, for "lonsdaleite" there should be discrete *h0l* reflections in <010> SAED projections, but they have not been observed[5]. Although features such as the 0.412-nm spacings on HRTEM images[4] and the reported distribution of reflections on FFTs[6-7] have been attributed to "lonsdaleite," they are inconsistent with its crystal structure. In addition, the reported *hk0* reflections in <001> SAED projections[6, 8-10] and HRTEM images[5] are not unique to "lonsdaleite" but also match those of graphite.

Supplementary References

1. Lábár, J. L. Electron diffraction based analysis of phase fractions and texture in nanocrystalline thin film, Part I: Principles. *Microsc. Microanal.* **14**, 287-295 (2008).

2. Guenette, M. *et al.* NEXAFS spectroscopy of CVD diamond films exposed to fusion relevant hydrogen plasma. *Diam. Rel. Mat.***34**, 45-49 (2013).

3. Kurdyumov, A.V., Britun, V. F., Yarosh, V. V., Danilenko, A. I. & Zelyavskii V. B. The influence of shock compression conditions on the graphite transformations into lonsdaleite and diamond. *J. of Superhard Mater.* 34, 19-27 (2012).

4. Kulnitskiy, B., Perezhogin, I., Dubitsky, G. & Blank, V. Polytypes and twins in the diamond-lonsdaleite system formed by high-pressure and high-temperature treatment of graphite. *Acta Crystallogr. Sect. B-Struct. Sci.* 69, 474-479 (2013).

5. Daulton, T. L., Eisenhour, D. D., Bernatowicz, T. J., Lewis, R. S. & Buseck, P. R. Genesis of presolar diamonds: comparative high-resolution transmission electron microscopy study of meteoritic and terrestrial nano-diamonds. *Geochim. Cosmochim. Acta* **60**, 4853-4872 (1996).

6. Israde-Alcantara, I. *et al.* Evidence from central Mexico supporting the Younger Dryas extraterrestrial impact hypothesis. *Proc. Natl. Acad. Sci. U.S.A.* **109(13)**, E738-E747 (2012).

7. Kumar, A. *et al.* Formation of nanodiamonds at near-ambient conditions via microplasma dissociation of ethanol vapour. *Nat. Commun.* **4,** 2618 (1-8) (2013).

8. Kennett, D. J. *et al.* Shock-synthesized hexagonal diamonds in Younger Dryas boundary sediments. *Proc. Natl. Acad. Sci. U.S.A.***106**, 12623-12628 (2009).

9. Kvasnytsya, V. *et al.* New evidence of meteoritic origin of the Tunguska cosmic body. *Planetary and Space Science* **84**, 131-140 (2013).

10. Nakamuta, Y. & Toh, S. Transformation of graphite to lonsdaleite and diamond in the Goalpara ureilite directly observed by TEM. *Am. Mineral.* **98**, 574-581 (2013).